REVISION AND RECALIBRATION OF EXISTING SHOCK CLASSIFICATIONS FOR QUARTZOSE ROCKS USING LOW SHOCK PRESSURE RECOVERY EXPERIMENTS (2.5-20 GPA) AND MESO-SCALE NUMERICAL MODELING. A. Kowitz[1,2], N. Güldemeister[1,2], R.T. Schmitt[1], W.U. Reimold[1,3], K. Wünnemann[1] and A. Holzwarth[4]; [1]Museum für Naturkunde, Leibniz-Institut für Evolution und Biodiversitäts-forschung, Invalidenstrasse 43, 10115 Berlin, Germany. [2] Freie Universität Berlin, Institut für Geologische Wissenschaften, Malteserstrasse 74-100, 12249 Berlin, Germany. [3]Humboldt Universität zu Berlin, Unter den Linden 6, 10099 Berlin, Germany. [4]Ernst-Mach-Institut, Am Christianswuhr 2, 79400 Kandern, Germany. E-mail: astrid.kowitz@mfn-berlin.de.

Introduction: The identification of impact craters formed in porous and wet sedimentary rocks, such as sandstone, on the basis of recognition of shock deformation features is a complex task. Most of the impacted target material is only weakly shocked, especially in the case of eroded remnants of impact structures or in small craters. There is a serious lack of diagnostic shock features, especially for the low shock-pressure range, which is addressed in this project focusing on shock deformation experimentally generated in dry and water saturated sandstones and for comparison in a quartzite, at shock-pressures from 2.5 to 20 GPa. We aim at establishing a shock classification scheme for porous, quartz-bearing rocks.

The *laboratory impact experiments* were accompanied by *meso-scale numerical modeling* in order to quantify processes beyond the optical and electron optical observational capabilities.

Methods: Four series of *shock recovery experiments* [1,2] were conducted with cylinders (Ø 1.5 cm, length 2 cm) of i) dry Seeberger sandstone L3 (layer 3; grain size: ~0.10 mm, porosity: 25-30 vol.%, quartz content: ~89 vol.%, pore size: 20-100 µm), ii) dry Seeberger sandstone L5 (layer 5; grain size: ~0.17 mm, porosity: 12-19 vol.%, quartz content: ~87 vol.%, pore size: 10-100 µm), iii) near-complete water-saturated Seeberger sandstone L3, and iv) quartzite (grain size: ~0.05-0.2 mm, porosity: <0.5 vol.%, quartz content: ~98 vol.%). The shock recovery experiments (Fig. 1a) were carried out with a high-explosive driven flyer plate set-up; generating a plane shock wave propagating into the sandstone cylinder [3]. To avoid multiple reflections of the shock wave within the sample material and to reach the desired pressures of 2.5 to 20 GPa, the impedance method was used [3].

Numerical model: To simulate shock wave propagation, the multi-material, multi-rheology hydrocode iSALE [4] coupled with the ANEOS for quartzite [5] and a virtual experimental set-up (Fig. 1b) similar to that used in the actual experiments was employed. Meso-scale modeling investigated the effects at individual pore spaces to obtain a better understanding of shock wave propagation through a heterogeneous material and of the processes associated with shock-induced pore-space collapse. A quantification of localized pressure amplification due to pore collapse was performed [6].

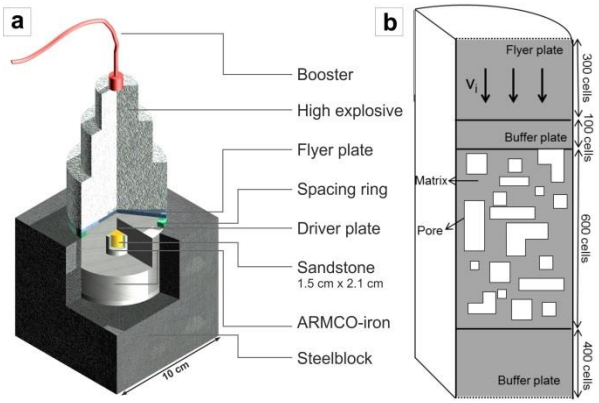

Fig. 1. (a) Experimental set-up for the shock recovery experiments. (b) Illustration of the meso-scale model set-up including the sample with a defined number of randomly distributed pores.

Results: A combination of shock recovery experiments and numerical modeling of shock deformation in the low pressure range from 2.5 to 20 GPa for the four experimental series provides new, significant insights. The general appearance of the recovered sample material from the four experimental series is shown in comparison to the unshocked source material in Fig. 2, which illustrates that there is an increase of deformation (increasing width and decreasing length of the samples) with increasing pressure - as well as with increasing porosity.

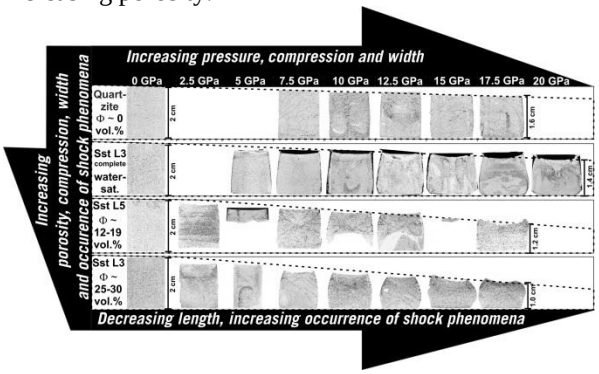

Fig. 2. Thin section scans of the four experimental series cut parallel to the propagation direction of the shock front and through the center

of the sample cylinder. At left margin: unshocked samples for comparison; to the right: experimentally shocked samples with increasing shock pressure.

The experiments clearly show that shock compression of porous sandstone results in a strongly heterogeneous distribution of different shock features that, in non-porous rocks, occur in a distinct sequence of progressive shock deformation.

(1) For *non-porous quartz-feldspathic rocks* the traditional classification scheme of [7] is well suitable. Shock experiments with our quartzite and, earlier, with Hospital Hill Quartzite [8] show that slight changes in pressure calibration are necessary for this material. The onset of planar deformation feature (PDF) formation in quartz in polycrystalline rocks seems to be at higher shock pressures than in single crystals, and occurs at 17.5-20 GPa. The formation of diaplectic quartz glass starts in quartzite, in comparison to single quartz crystals, already at lower pressures (~30 GPa).

(2) For *water-saturated quartzose rocks* in the pressure range up to 20 GPa a cataclastic texture (microbreccia) is typical. This microbreccia does not show formation of PDF up to 20 GPa but rare diaplectic quartz glass/SiO_2 melt (lechatelierite) formation starts at 15 GPa and increases to ~1 vol.% at 20 GPa.

(3) For *porous quartzose rocks* the following sequence of shock features is observed: i) crushing of pores; ii) intense fracturing of quartz grains; and iii) increasing formation of diaplectic quartz glass/SiO_2 melt replacing fracturing.

Discussion: The combination of new shock experiments and numerical modeling provides significant insights into the shock processes in the low shock pressure regime (2.5-20 GPa) for porous, dry and water-saturated sandstones, and quartzite. Polycrystallinity of a rock already changes a shock calibration, as illustrated by the experiments with quartzite in comparison to calibrations based on shock recovery experiments with single crystals of quartz. Therefore, the calibration of the shock classification system for non-porous quartzo-feldspathic rocks by [7] needed to be changed somewhat.

Porosity causes a very strong effect on the formation of shock deformation features. Increasing porosity, in comparison to non-porous quartzite or water-saturated sandstone, leads to:

1. Comparatively stronger deformation of targets;
2. stronger mechanical damage, as expressed by relatively higher numbers of fractures that, then decrease at comparatively lower shock pressures;
3. replacement of fracturing by melting at comparatively lower shock pressures; and formation of higher amounts of diaplectic quartz glass and/or SiO_2 melt, and onsets at distinctly lower shock pressures.

Confirmed by numerical modeling, all these observations are a result of pore-crushing processes leading to local pressure amplifications of up to 4 times the shock pressures attained in non-porous rock [2,6] and, therefore, to an earlier onset of formation of glass phases, melt and high-pressure phases. These findings required a revision and recalibration of the previous shock classification scheme for porous sandstone [9]. The calibration of shock stages strongly depends on porosity before impact, which is visualized in a porosity vs. shock pressure diagram by isolines separating the different shock stages (Fig. 3). Thus, for shock classification and shock calibration of porous natural samples, the original porosity (and water content) of the unshocked material has to be determined before shock calibration can be attempted.

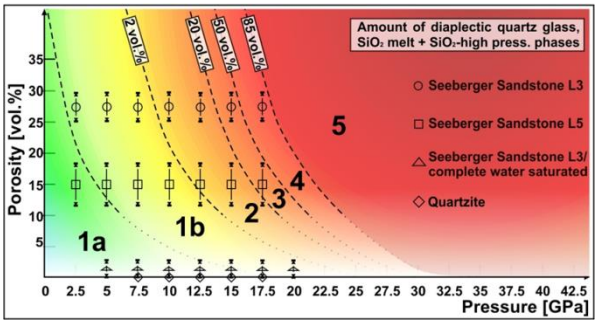

Fig. 3. Pressure calibration of shock stages 1a to 5 for porous sandstone versus porosity. The isolines of the amounts of diaplectic quartz glass, SiO_2 high pressure phases, and SiO_2 glass represent the limits between shock stages 1b to 5. The boundary between shock stages 1a and 1b is defined by the complete closure of pore space. The arrow lines at each datapoint represent the range of porosity for the individual targets of the shock recovery experiments.

Acknowledgements

This work was funded by DFG research unit FOR-887 (MEMIN) projects WU 355/6-1 and RE 528/8-2 and 8-3.

References

[1] Kowitz A. et al. (2013) *MAPS* 48, 99-114. [2] Kowitz A. et al. (2013) EPSL 384, 17–26. [3] Stöffler D. and Langenhorst F. (1994) *MAPS*, 29, 155-181. [4] Wünnemann K. et al. (2006) *Icarus* 180, 514–527. [5] Melosh H.J. (2007) *MAPS*, 42, 2035–2182. [6] Güldemeister N. et al. (2013) *MAPS* 48, 115-133. [7] Stöffler D. (1984) *Noncrystalline Solids* 67, 465-502. [8] Reimold W.U. and Hörz F. (1986) *Geocongress 86*, 53-57, Geol. Soc. S. Afr., Johannesburg. [9] Kieffer S. W. et al. (1976) *Contrib. Mineral. Petrol*., 76, 41-93.